Implementation of Blade Element Momentum/Vortex Methods for the Design of Aero Engine Propellers

Research report 2017:06

Implementation of Blade Element Momentum/Vortex Methods for the Design of Aero Engine Propellers

by

ALEXANDRE CAPITAO PATRAO

Mechanics and Maritime Sciences (M2)
CHALMERS UNIVERSITY OF TECHNOLOGY
Göteborg, Sweden, 2017

Implementation of Blade Element Momentum/Vortex Methods for the Design of Aero Engine Propellers

ALEXANDRE CAPITAO PATRAO

Research report 2017:06

Division of Fluid Dynamics
Department of Mechanics and Maritime Sciences
CHALMERS UNIVERSITY OF TECHNOLOGY
SE-412 96 Göteborg
Sverige
Telephone +46 (0)31 772 1000

Implementation of Blade Element Momentum/Vortex Methods for the Design of Aero Engine Propellers

Alexandre Capitao Patrao

2017-11-27
Chalmers University of Technology
Department of Mechanics and Maritime Sciences
Division of Fluid Mechanics
capitao@chalmers.se
alexandre.capitao.patrao@gmail.com

TABLE OF CONTENTS

1 INTRODUCTION

This report outlines the theory and methodology used in the Chalmers in-house propeller design code OPTOPROP. The design code was developed in order to enable the design of propeller blades for aircraft engines, particularly for open rotor engines. A literature study of existing propeller design and analysis methods is done, and a number of promising design methods based on the Blade Element-Momentum and Blade Element-Vortex methods are implemented. An in-house variant of these design and analysis methods is also derived which can account for non-uniform inflow to the propeller. The methods are validated against experimental results from literature and numerical (CFD) simulations and show good accordance in their trends. The design methods would benefit from calibration since the thrust obtained thrust values from CFD are slightly under-predicted relative to OPTOPROP. Nevertheless, the design program has shown itself to be very useful for the design and optimization of propellers and open rotor blades.

2 LITERATURE REVIEW

A literature study was conducted regarding methods on how to design and analyze propellers, with methods ranging in complexity from Blade Element Methods (BEM) to Panel Methods. The main idea of this literature study is to investigate what kind of tools, methodology, and reasoning are being used for propeller design.

2.1 ZONDERVAN

The author gives a small review [1] of the modelling challenges associated with propellers, starting with the simplest models all the way to Euler methods. The main points are:

- Propeller design for open rotors is complicated due to the complex shape of the blades, transonic operating regime, and high blade loading (at least during take-off).
- Highly loaded propeller blades experience non-linear effects, and will not have the ordered helical wake structures common for lightly loaded propellers. Unfortunately, this paper does not mention what can be considered light or heavy loading. Only direct reference is that loading is high during take-off.
- Any distortion (high loading, low forward speed, wings, nacelles, engine angle-of-attack, etc) of the helical wake structures complicate the propeller analysis.
- When designing for a large number of blades, cascade effects has to be considered.
- Nacelle boundary layers are usually omitted when analyzing propellers with methods simpler than CFD.
- Some sort of tip model has to be used in order to account for the effects of the tip vortex on blade design and performance.
- *Momentum Theories* (Rankine, Froude) are very rough models. The blade is treated as a discontinuity where thrust is produced.
- The *Blade Element Method* does not include the effects of the wake on the blade.
- The *Momentum-Blade Element Theory* models both the blade and wake, and can also include a tip loss factor (commonly the Prandtl tip loss factor).
- *Vortex methods* have a wake with a prescribed shape, and does not include wake contraction. The induced axial velocities at the disk are half of the values in the downstream wake. Goldstein [2] and Theodorsen [3] made further developments to these theories in the 1920's and 1940's.
- Theodorsen showed that the important factor for when designing an optimum propeller, is that the axial velocity increase (called *displacement velocity*) of the wake is constant with respect to radius, which in the end results in a helical wake. This idea is similar to the constant downwash of an elliptically loaded wing, which is the optimum for a wing with a tip vortex.
- Using vortex methods for off-design analysis is only valid very close to the design point, since at off-design the wake no longer adheres to its helical "optimum" shape. Any condition where the wake does not behave in this

helical way (take-off, landing, high loading, and highly 3D flow) will lead to larger discrepancies between the vortex methods and reality.

2.2 McCormick

A second review of propeller design and analysis methods can be found in a book by McCormick [4]. Several concepts are similar to the ones mentioned by Zondervan, so only the additional ones will be mentioned here:

- Vortex methods assume that the induced velocities at the disk are perpendicular helical vortex sheets that extend from the propeller blade sections.
- The *Betz condition* for an optimum propeller is that the pitch of the helical vortex sheets in the far wake have the same value.

$$p_{wake} = 2\pi r tan(\phi_W) = const$$

- The circulation at the blade and in the far wake must be the same.

2.3 Larrabee

This paper [5] discusses a straight-forward way of obtaining propeller designs for the *Minimum Induced Loss* condition, which also adheres to the Betz condition.

- Based on the Vortex methods.
- Uses the Prandtl tip loss factor.
- Larrabee models the wake as an infinite trailing vortex sheet, and uses the concept of constant displacement velocity (similar to wings with constant downwash).
- One unfortunate approximation made by Larrabee is the one of *light loading* which neglects the induced velocities at the propeller plane, which simplifies some of his equations. This also leads to the design and analysis methods in his paper to give different results at the design point.
- The displacement velocity is solved for directly from a second order polynomial, and the only input needed is either the required power or thrust.

2.4 Adkins

Builds [6] on the Theodorsen methodology, but is much simpler to implement.

- Conceptually similar to the Larrabee paper, but without any light loading assumptions.
- Uses the Prandtl tip loss factor and Betz condition for optimum propellers.
- Connects the displacement velocity to the Betz condition and shows that the displacement velocity is constant with respect to radius.
- The displacement velocity is solved iteratively from a second order polynomial with pre-specified thrust or power. Larrabee could solve it directly, but only because of his light loading assumption.
- The design and analysis methods of the paper give virtually the same results for the same propeller design.

2.5 Drela

A student of Larrabee which has written his own propeller analysis code QPROP. The theory behind QPROP [7] is available online, and can be briefly described in the following way:

- Larrabee and Adkins use variants of the *Momentum-Blade Element Theory* together with a prescribed wake. Drela instead uses the equations for describing what happens at the blade element to calculate the circulation produced there, and equals it to circulation of the wake.

- The blade and the wake are connected with an unreferenced equation, which relates the tangential velocity in the blade with the circulation in the wake. Unfortunately no source or derivation of this equation is given.
- Drela assumes that the induced velocities at the blade are perpendicular to the velocity in the relative frame.
- The essential part of Drela's code is that it takes an existing propeller geometry and an uninduced flowfield, and iterates on the induced velocities at the blade until the circulation in the blade matches what it is in the wake.
- Drela has used a very clever parametrization of the velocities in the blade element, which allows the program to quickly converge on a result.
- For minimum induced loss design, some variables (chord, blade angle, sectional induced efficiency) are set to vary in order to find a target thrust or power.
- Drela shows that for a minimum induced loss propeller, the induced efficiency for each blade section is independent of blade radius. A higher induced efficiency gives lower thrust, while a lower induced efficiency gives higher thrust, so the efficiency acts a lever in order to reach a target thrust.

2.6 Bechet and Negulescu (2011)

This paper [8] is a basis for the Negulescu paper below, and contains mainly:

- Explanation of the design process used for the AI-PX7 open rotor configuration.
- The lifting line method is used, but is only valid for preliminary design of blades. It is still important because it captures a large part of the physics.
- Initial design of the AI-PX7 was done with the lifting line tool LPC2, and then performing small changes to the geometry and simulating it using CFD. The chord, sweep, camber, and thickness are varied over relative small ranges and the trends on performance are observed.

2.7 Negulescu (2013)

A good overview [9] of the main parameters influencing the design and performance of a CROR. The design used in the same as in the paper by Bechet [8] (Negulescu is a co-author). The author gives sensible parameter ranges for number of blades, rotor spacing, rear rotor clipping, etc.

2.8 Gonzalez-Martino (2013)

The authors [10] compare results between CFD and an unsteady lifting line tool called HOST to compare a generic open rotor configuration (AI-PX7) at Mach 0.73. The results for the lifting line are very well aligned with the CFD, with the thrust differing only 1.5%. The lifting line tools seems quite capable, but is more complex to implement than the BEM and vortex methods.

The AI-PX7 blade and nacelle configuration has been mentioned in another paper by Negulescu [8], in which blade parameter sweeps are done with a lifting line tool called LPC2.

2.9 Kobayakawa (1985)

A sophisticated and complex vortex lattice method is used in this paper [11] for the simulation of the NASA SR-3 propeller. Unfortunately, this particular method is only suitable for tip speeds below Mach 1 and cannot handle transonic flow. The method accounts both for sweep and lean, but is incompressible. The results agree well with experiments, but the performance can only be calculated for axial Mach numbers below 0.6.

3 THEORY

Based on the literature study, it was decided to start with the simpler BEM and vortex methods because of their approachability and simplicity in comparison with the lifting line and vortex lattice methods.

3.1 COMMON TERMINOLOGY

3.1.1 Blade element velocities

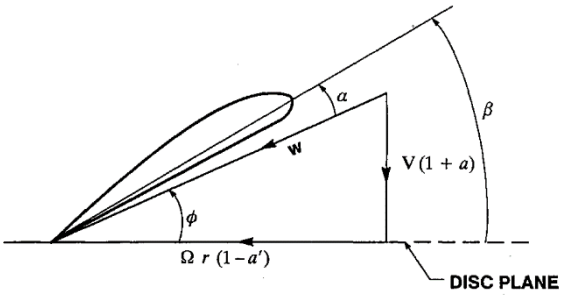

Figure 1 - Propeller blade section including induced velocities and flow angle. Source: Adkins [6].

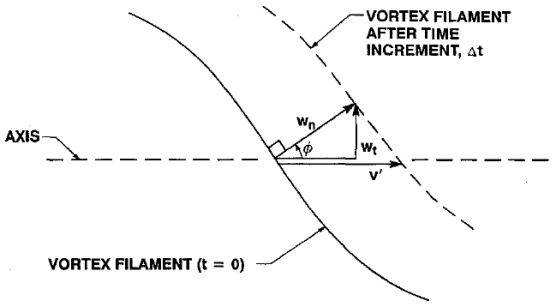

Figure 2 – Propeller wake far downstream. Source: Adkins [6].

The induction factors a and a' denote the induced *axial* and *tangential* velocities at the blade element, giving velocities and flow angle at the blade element corresponding to:

$$W_a = V(1+a) \tag{1}$$

$$W_t = \Omega r(1-a') \tag{2}$$

$$W = \sqrt{W_a^2 + W_t^2} \tag{3}$$

$$\tan\phi = \frac{V(1+a)}{\Omega r(1-a')} \tag{4}$$

This is done assuming that the inflow is uniform with velocity V and no upstream induced tangential velocities (from other propellers or nacelles).

3.1.2 Wake velocities

The axial velocity displacement v' in the far wake is shown in Figure 2. It is common to rewrite it using an *axial velocity displacement ratio* $\zeta = v'/V$. For the Larrabee and Adkins theories, the vortex sheet is assumed to move with same angle as the flow angle at the propeller blade section.

3.1.3 Prandtl tip loss factor

The Prandtl tip loss factor is a simple model that accounts for the effects of a tip vortex on the flow passing through it. This is done by decreasing the amount of momentum that the blade tip can impart on the flow at the blade tip. The definition is as displayed below:

$$F = \frac{2}{\pi}\operatorname{acos} e^{-f} \tag{5}$$

Where the factor f is defined differently for the various methods in this article.

3.2 METHODOLOGY OF LARRABEE

The foundation of the methodology of Larrabee rests mainly on the following concepts:

- Blade element force calculation based on induced axial a and tangential velocity factors (a and a', see Figure 1).
- Prescribing a shape for the propeller helical wake (Figure 2).
- The Betz condition for an optimum propeller is expressed through an axial velocity displacement (v'), which is constant with respect to radius.
- Light loading assumption, which neglects wake contraction, and assumes that the induced velocities are small relative to the magnitude of the axial and rotational non-induced velocities.
- The flow angle of the helical wake is assumed to identical to the one at the blade section.

3.2.1 Wake equations

The helical wake is modelled as a vortex sheet extending from the propeller section, and its tangential velocity is determined by (see Figure 1):

$$w_t = w_n \sin\phi = v' \sin\phi \cos\phi \tag{6}$$

This is the tangential velocity of the helical wake that the whole propeller produces, and varies with radius. The circulation can then be calculated for annular strips of the wake as follows:

$$B\Gamma = 2\pi r w_t F = 2\pi r v' \sin\phi \cos\phi \, F \tag{7}$$

Where F is the Prandtl tip loss factor, and Γ is the circulation produced by each blade. The trigonometric terms can be rewritten using the velocities in Figure 1, and assuming light loading one can neglect the induced velocities to obtain:

$$\sin\phi = \frac{1}{\sqrt{1+x^2}} \qquad \cos\phi = \frac{x}{\sqrt{1+x^2}} \qquad x = \Omega r / V \tag{8}$$

This is a rather major simplification (since Adkins later showed it to be unnecessary), which will later lead to the Larrabee design and analysis routines returning slightly different results. Combining equation (7) and (8):

$$\frac{B\Gamma\Omega}{2\pi V v'} = \frac{x^2}{1+x^2} F = G \tag{9}$$

Where:

$$F = \frac{2}{\pi}\operatorname{acos}(e^{-f}) \qquad f = \frac{B}{2}\frac{\sqrt{\lambda^2+1}}{\lambda}(1-\xi) \qquad \lambda = \frac{V}{\Omega R} \tag{10}$$

The nondimensional radius is denoted with ξ. Equation (9) above can be rewritten for the blade circulation in terms of the *axial velocity displacement ratio* ζ:

$$\Gamma = \frac{2\pi V v' G}{B\Omega} = \frac{2\pi G}{B\Omega} V^2 \zeta \tag{11}$$

3.2.2 Blade section equations

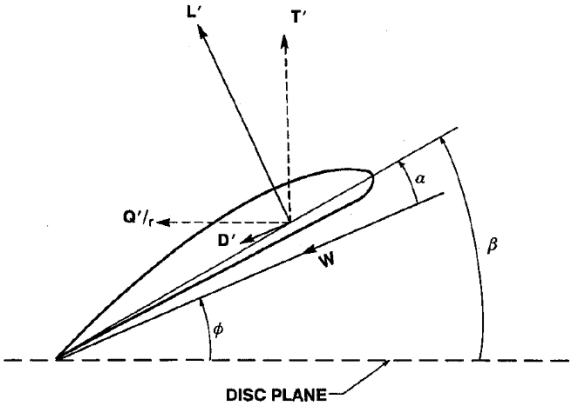

Figure 3 - Forces acting on a blade element. Source: Adkins (1994).

Blade thrust sectional thrust $T' = dT/dr$ can be written with the help of Figure 3 :

$$T' = L'\cos\phi - D'\sin\phi = L'\cos\phi(1 - \epsilon\tan\phi) \tag{12}$$

Where ϵ is the drag-to-lift ratio for the airfoil section. The trigonometric terms can be rewritten using the relations in equation (8). The lift term can be written with the Kutta-Joukowski theorem using the blade circulation:

$$T' = L'\cos\phi(1 - \epsilon\tan\phi) = B\rho W\Gamma\cos\phi(1 - \epsilon\tan\phi) \tag{13}$$

$$T' = B\rho\Gamma\Omega\mathrm{r}(1 - a')(1 - \epsilon\tan\phi) \tag{14}$$

The tangential velocity induction factor a' is assumed to be half the value of the tangential velocity in the wake w_t:

$$a' = \frac{1}{2}\frac{w_t}{\Omega r} = \frac{1}{2}\frac{v'\sin\phi\cos\phi}{\Omega r} = \{eq.(8)\} = \frac{1}{2}\,\zeta\,\frac{1}{1+x^2} \tag{15}$$

$$\rightarrow T' = B\rho\Gamma\Omega\mathrm{r}\left(1 - \frac{1}{2}\,\zeta\,\frac{1}{1+x^2}\right)(1 - \epsilon\tan\phi) \tag{16}$$

The circulation Γ is taken from the wake (eq. (11)), and the $\tan\phi$ term is simplified with equation (8):

$$\rightarrow T' = 2\pi r\rho G V^2\zeta\left(1 - \frac{1}{2}\,\zeta\,\frac{1}{1+x^2}\right)\left(1 - \frac{\epsilon}{x}\right) \tag{17}$$

The interesting result here is that the velocity displacement ratio ζ is constant with respect to the radius, and therefore the entire expression above can be integrated from hub to blade tip. This results in the blade thrust on the left hand side, and a number of integrals on the right hand side which will form the coefficients of a second order equation with ζ as the variable. In this way, one can specify thrust, and obtain the needed velocity displacement ratio.

3.2.3 Constraint equations

The design will now be constrained to a particular thrust or power. For this document only thrust will be used, but power can easily be implemented. First, the sectional thrust is rewritten with the help of the thrust coefficient T_c:

$$T_C = \frac{2T}{\rho V^2\pi R^2} \rightarrow T' = \frac{dT}{dr} = \frac{1}{2}\rho V^2\pi R\frac{dT_c}{d\xi} \tag{18}$$

Where ξ is the dimensionless radius. Substituting equation (18) into (17):

$$\frac{dT_c}{d\xi} = 4\xi G\zeta\left(1-\frac{\epsilon}{x}\right) - 2\xi G\zeta^2\left(\frac{1-\epsilon}{x^2+1}\right) \tag{19}$$

Integrating this expression from hub ($\xi_1 = HTR$) to tip ($\xi = 1$), will allow the velocity displacement to be solved for given a thrust coefficient T_c:

$$\zeta = \frac{I_1}{2I_2}\left(1+\sqrt{1-\frac{4I_2T_c}{I_1^2}}\right) \tag{20}$$

Where the integrals I_1 and I_2 can be computed directly:

$$I_1 = \int_{\xi_1}^{\xi_2} 4\xi G\left(1-\frac{\epsilon}{x}\right)d\xi \qquad\qquad I_2 = \int_{\xi_1}^{\xi_2} 2\xi G\left(\frac{1-\frac{\epsilon}{x}}{x^2+1}\right)d\xi \tag{21}$$

Knowing ζ allows the calculation of the induction factors. The tangential induction factor is found with equation (15), and the axial induction factor is assumed to be half of the wake axial velocity:

$$a = \frac{1}{2}v'\cos^2\phi = \{eq.(8)\} = \frac{1}{2}\,\zeta V\frac{x^2}{1+x^2} \tag{22}$$

The flow angle becomes according to Figure 1:

$$\phi = \operatorname{atan}\left(\frac{V(1+a)}{\Omega r(1-a')}\right) \tag{23}$$

3.2.4 Larrabee design algorithm

Below is a short description of the algorithm based on the Larrabee method. Blade diameter, hub radius, axial velocity, rotational velocity, and number of blades have to be set before initiating design.

Larrabee design algorithm

1. Specify T_C and design lift coefficient distribution $c_l = f(r)$.
2. Calculate:
    a. The Prandtl tip loss factor with eq. (10).
    b. The G function with eq. (9).
    c. The coefficient of drag c_d and angle of attack α from airfoil data. Allows calculation of $\epsilon = c_d/c_l$.
3. Calculate the integrals I_1 and I_2 with equation (21).
4. Solve the polynomial for ζ.
5. Calculate the induction factors a and a' using equations (15) and (22). The total velocity W can also be calculated.
6. Calculate the flow angle ϕ. The blade angle can be calculated through $\beta = \phi + \alpha$.
7. Calculate dT/dr and dQ/dr and integrate to obtain thrust, torque, power, and efficiency.
8. The circulation can be calculated with equation (11), which then together Kutta-Joukowski equation for lift yields the chord of the blade section:

$$\rho W\Gamma = \frac{1}{2}\rho W^2 c c_l \rightarrow c = \frac{2\Gamma}{W c_l}$$

If Reynolds and Mach numbers are needed in order to estimate the blade section c_l, c_d, and α, then one should iterate from point 2 to 8, and update the Reynolds and Mach numbers with the obtained total velocity W and chord. This should be done until the drag-to-lift ratio ϵ reaches convergence.

Chord is in this case an output variable since the lift distribution is pre-specified. The lift coefficient distribution can be iterated on to yield a wanted chord distribution.

3.2.5 Larrabee analysis algorithm

If the blade design already exists, then Larrabee provides another method that can be used to analyze the performance given a particular flowfield. This method will not be elaborated on further, since Adkins uses the same method, and is presented in the next section.

3.3 Methodology of Adkins

The methodology used by Adkins is similar to Larrabee's, but introduces some additional concepts:

- Incorporates momentum equations between far upstream and far downstream of the blade, which is consistent with Actuator Disk Theory.
- Does not use the light loading assumption in which the induced velocities are assumed small relative to the magnitude of the freestream velocities (axial and tangential).

3.3.1 Momentum equations

The air flowing through an annular volume extending from far upstream, through a blade section with length dr, and continuing far downstream, will experience a force and torque equal to the thrust and torque of the blade. This can be written for the sectional thrust and torque as follows:

$$T' = 2\pi r \rho V (1 + a)(2VaF) \tag{24}$$

$$\frac{Q'}{r} = 2\pi r \rho V (1 + a)(2\Omega r a' F) \tag{25}$$

The terms in the second parenthesis are the changes in axial and tangential velocity that the air experiences when travelling through the annular streamtube.

3.3.2 Wake equations

The equation for the circulation in the wake is the same as in Larrabee's method.

$$\Gamma = \frac{2\pi V v' G}{B\Omega} = \frac{2\pi G}{B\Omega} V^2 \zeta \tag{26}$$

$$G = Fx \cos\phi \sin\phi \tag{27}$$

The Prandtl tip loss factor is defined slightly different:

$$F = \frac{2}{\pi} \operatorname{acos}(e^{-f}) \qquad f = \frac{B}{2}(1 - \xi)\frac{1}{\sin\phi_T} \qquad \phi_T = \operatorname{atan}\left(\lambda\left(1 + \frac{\zeta}{2}\right)\right) \tag{28}$$

3.3.3 Blade section equations

The blade section equations are identical to the ones used by Larrabee:

$$T' = L' \cos\phi (1 - \epsilon \tan\phi) \tag{29}$$

$$\frac{Q'}{r} = L' \sin\phi \left(1 + \frac{\epsilon}{\tan\phi}\right) \tag{30}$$

3.3.4 Induction factors

The sectional lift term is replaced by the Kutta-Joukowski equation for lift together with eq. (11):

$$L' = B\rho W\Gamma = \frac{2\pi\rho V^2 W\zeta G}{\Omega} \tag{31}$$

Which is then inserted into the blade section thrust and torque equations (29) and (30):

$$T' = \frac{2\pi\rho V^2 W\zeta G}{\Omega}\cos\phi(1 - \epsilon\tan\phi) \tag{32}$$

$$\frac{Q'}{r} = \frac{2\pi\rho V^2 W\zeta G}{\Omega}\sin\phi \left(1 + \frac{\epsilon}{\tan\phi}\right) \tag{33}$$

In order to get expressions for the axial and tangential induction factors, the momentum equations (24) and (25) are equaled to the expressions for blade thrust and torque above, and solved for a and a'.

$$a = \frac{\zeta}{2}\cos^2\phi\,(1 - \epsilon\tan\phi) \tag{34}$$

$$a' = \frac{\zeta}{2x}\sin\phi\cos\phi \left(1 + \frac{\epsilon}{\tan\phi}\right) \tag{35}$$

3.3.5 Proof of minimum induced loss

The Betz condition for a propeller or windmill with *minimum induced loss* (MIL) is that the wake behaves as a helicoid, and that the expression $r\ tan\ \phi$ is constant with respect to radius (according to Adkins). A proof of the statement that the velocity displacement ratio $\zeta = v'/V$ is constant with radius for a MIL propeller will be obtained in this section. Starting with equation (34) and (35) the drag-to-lift ratio ϵ can be eliminated:

$$\left(1 - \frac{2a}{\zeta\cos^2\phi}\right)\frac{1}{\tan\phi} = \left(\frac{2xa'}{\zeta\cos\phi\sin\phi} - 1\right)\tan\phi \tag{36}$$

After some manipulation, the following is obtained:

$$\frac{\zeta}{2} = a + xa'\tan\phi \tag{37}$$

$$\tan\phi = \frac{V(1+a)}{\Omega r(1-a')} \rightarrow (37) \tag{38}$$

$$\rightarrow r\tan\phi = \frac{V}{\Omega}\left(\frac{\zeta}{2} + 1\right) \tag{39}$$

Since the Betz condition states that the left hand side must be constant with respect to radius for MIL propeller, so must the right hand side, including the velocity displacement ratio ζ. Rewriting the equation above in a more convenient form:

$$\tan\phi = \frac{\lambda}{\xi}\left(1 + \frac{\zeta}{2}\right) \tag{40}$$

3.3.6 Constraint equations

As was the case for Larrabee, the design must be constrained by setting either a thrust or torque. The approach is similar, and will not be treated in any great detail here, but instead outlined:

$$\zeta = \frac{I_1}{2I_2}\left(1 + \sqrt{1 - \frac{4I_2 T_c}{I_1^2}}\right) \tag{41}$$

$$\frac{dI_1}{d\xi} = 4\xi G(1 - \epsilon \tan\phi) \qquad \frac{dI_2}{d\xi} = \frac{\lambda}{2\xi}\frac{dI_1}{d\xi}\left(1 + \frac{\epsilon}{\tan\phi}\right)\sin\phi\cos\phi \tag{42}$$

The expressions in eq. (42) above are written in un-integrated form for clarity. After integrating both, the velocity displacement ratio can be calculated. One difference relative to the Larrabee method is the inclusion of the flow angles, which makes this method iterative instead of direct.

3.3.7 Reynolds number calculation

The Reynolds number is needed for the correct calculation of blade section lift and drag coefficients. Equaling the lift produced by a blade section with the Kutta-Joukowski equation gives:

$$\frac{1}{2}\rho W^2 c c_l = \rho W \Gamma \tag{43}$$

With equation (26) the term Wc can be written as follows:

$$Wc = \frac{4\pi\lambda G V R \zeta}{c_l B} \tag{44}$$

3.3.8 Adkins design algorithm

Below is a short description of the algorithm based on the Adkins method. Blade diameter, hub radius, axial velocity, rotational velocity, number of blades, thrust coefficient T_C, and design lift distribution have to be set before initiating design.

Adkins design algorithm

1. Set an initial guess for ζ (equal to zero works).
2. Calculate:
    a. The Prandtl tip loss factor with eq. (28).
    b. The flow angle for each radial position with eq. (40).
    c. The G function with eq. (27).
    d. The product of total velocity W and chord, which is used to calculate Reynolds number.
3. Calculate coefficient of drag c_d and angle of attack α from airfoil data. Allows calculation of $\epsilon = c_d/c_l$.
4. Calculate a and a', which gives the total velocity $W = V(1 + a)/\sin\phi$.
5. Calculate chord and blade angle $\beta = \phi + \alpha$.
6. Integrate the terms in eq. (42) and solve for ζ with eq. (41).
7. Go back to step 2 and Iterate until ζ converges on a final value.
8. Calculate dT/dr and dQ/dr in and integrate to obtain thrust, torque, power, and efficiency.

Mach number can be included for the airfoil sections, but will only be calculated after step 4, and it will only effect the next iteration.

Chord is in this case an output variable since the lift distribution is pre-specified. The lift coefficient distribution can be iterated on to yield a wanted chord distribution, exactly as with the Larrabee method.

3.3.9 Adkins analysis method

The method for analysis in Adkin's paper is very similar to the *Momentum-Blade Element Theory*. Starting with Figure 4, the blade element force coefficients c_x and c_y are written using the lift and drag coefficients, which are then used in expressions for sectional thrust and torque:

$$c_y = c_l(\cos\phi - \epsilon\sin\phi) \qquad c_x = c_l(\sin\phi + \epsilon\cos\phi) \tag{45}$$

$$T' = \frac{1}{2}\rho W^2 B c c_y \qquad \frac{Q'}{r} = \frac{1}{2}\rho W^2 B c c_x \tag{46}$$

By equaling equation (46) with the momentum equations (24) and (25), and solving for the induction factors a and a' results in two expressions:

$$a = \frac{\sigma c_y}{4F\sin^2\phi - \sigma c_y} \qquad a' = \frac{\sigma c_x}{4F\sin\phi\cos\phi + \sigma c_x} \qquad \sigma = \frac{Bc}{2\pi r} \tag{47}$$

The solidity of the blade is termed σ. The analysis algorithm is outlined below.

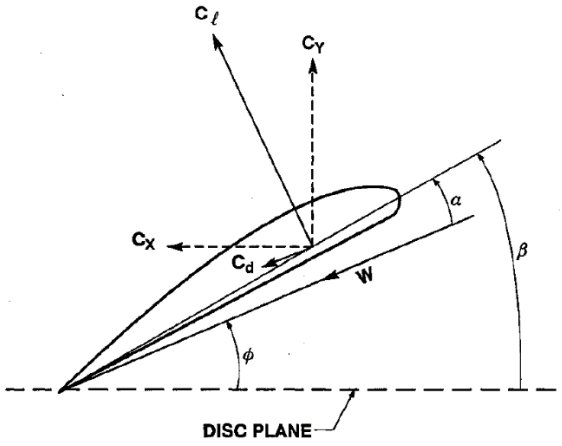

Figure 4 - Blade element force coefficients C_x and C_y. Source: Adkins (1994).

Adkins analysis algorithm

1. Set the initial guess for the flow angle. Use $\phi = \text{atan}(V/\Omega r)$.
2. Since the blade angle and flow angle are known, angle-of-attack can be calculated with $\alpha = \beta - \phi$.
3. Calculate airfoil coefficients c_l and c_d. If Reynolds and Mach numbers are needed, use either the initial values for velocity or the velocity from the previous iteration.
4. The Prandtl tip loss factor with eq. (28). Adkins suggests $\tan\phi_T = \xi\tan\phi$ for calculating ϕ_T for analysis.
5. Calculate the blade element force coefficients c_x and c_y with eq. (45).
6. Calculate the induction factors a and a' with eq. (47), which will give an update on the total velocity W.
7. Calculate a new flow angle:

$$\phi_{new} = \text{atan}\frac{V(1+a)}{\Omega r(1-a')}$$

8. Update the flow angle using a relaxation factor κ:

$$\phi = (1-\kappa)\phi_{old} + \kappa\phi_{new}$$

9. Back to step 2 and iterate until the flow angle has converged.

The Adkins design and analysis methods will return the same performance at the design point, which Larrabee's method could not achieve.

3.3.10 Extending the methodology of Adkins for upstream induced flow

The methodology of Adkins is essentially a *Momentum-Blade Element Theory* that is constrained by the Betz condition on the wake (i.e. the wake being helicoidal). In this section of the report, the author has derived an extension to Adkins method which incorporates upstream velocities that have been induced by either a nacelle or an upstream counter-rotating propeller, giving rise to a non-uniform inflow.

The design and analysis methods are based on the Adkins analysis algorithm, with modification to account for non-uniform upstream flow. The momentum equations are very similar to previous ones, but with a modification in the mass flow through the control volume (marked bold below):

$$T' = 2\pi r\rho V(\mathbf{1} + \boldsymbol{a} + \boldsymbol{a}_\infty)(2VaF) = 4\pi r\rho V^2 a(1 + a + a_\infty)F \tag{48}$$

$$\frac{Q'}{r} = 2\pi r\rho V(\mathbf{1} + \boldsymbol{a} + \boldsymbol{a}_\infty)(2\Omega r a'F) = 4\pi r^2\rho\Omega V a'(1 + a + a_\infty)F \tag{49}$$

The blade section velocities and are now defined in the following way:

$$W_a = V(1 + a + a_\infty) \qquad W_t = \Omega r(1 - a' - a'_\infty) \qquad W = \sqrt{W_a^2 + W_t^2} \tag{50}$$

If the upstream axial velocity is below the freestream velocity V, then $a_\infty < 0$. If an upstream rotor has produced swirl that is in the opposite direction of Ω, then $a'_\infty < 0$. If the momentum equations are equaled to the thrust and torque acting on the blade element (eq. (46)), one obtains equations of the induction factors that are very similar to eq. (47). The only difference is the inclusion of the upstream velocities:

$$a = \frac{(1 + a_\infty)\sigma c_y}{4F\sin^2\phi - \sigma c_y} \qquad a' = \frac{(1 - a'_\infty)\sigma c_x}{4F\sin\phi\cos\phi + \sigma c_x} \qquad \sigma = \frac{Bc}{2\pi r} \tag{51}$$

These equations will naturally become eq. (47) if the inflow is uniform. The analysis algorithm is outlined below.

Capitao analysis algorithm

1. Set the initial guess for the flow angle. Use $\phi = \text{atan}\big(V(1 + a_\infty)/\Omega r(1 - a'_\infty)\big)$.
2. Since the blade angle and flow angle are known, angle-of-attack can be calculated with $\alpha = \beta - \phi$.
3. Calculate airfoil coefficients c_l and c_d. If Reynolds and Mach numbers are needed, use either the initial values for velocity or the velocity from the previous iteration.
4. The Prandtl tip loss factor with eq. (28). Use the present flow angle at the tip as ϕ_T.
5. Calculate the blade element force coefficients c_x and c_y with eq. (45).
6. Calculate the induction factors a and a' with eq. (51), which will give an update on the total velocity W.
7. Calculate a new flow angle:

$$\phi_{new} = \text{atan}\frac{V(1 + a + a_\infty)}{\Omega r(1 - a' - a'_\infty)}$$

8. Update the flow angle using a relaxation factor κ:

$$\phi = (1 - \kappa)\phi_{old} + \kappa\phi_{new}$$

9. Back to step 2 and iterate until the flow angle has converged.

3.3.10.1 Proof of minimum induced loss

The analysis routine outlined above can only analyze existing blade geometries, and in order to find a propeller with minimum induced loss, the geometry needs to be modified (and then analyzed again). A MIL propeller with a uniform inflow respects the Betz condition by having a constant velocity displacement ratio ζ with respect to radius. A more general way to express the Betz condition is to use some sort of efficiency. Starting with the propeller efficiency for a propeller blade section:

$$\eta = \frac{VdT}{\Omega dQ} \tag{52}$$

Expanding the thrust and torque with the Kutta-Joukowski equation:

$$\frac{dT}{dr} = \frac{dL}{dr}(\cos\phi - \epsilon\sin\phi) = B\rho W\Gamma(\cos\phi - \epsilon\sin\phi) \tag{53}$$

$$\rightarrow \frac{dT}{dr} = B\rho\Gamma(W\cos\phi - \epsilon W\sin\phi) = B\rho\Gamma(W_t - \epsilon W_a) \tag{54}$$

$$\frac{1}{r}\frac{dQ}{dr} = \frac{dL}{dr}(\sin\phi + \epsilon\cos\phi) = B\rho W\Gamma(\sin\phi + \epsilon\cos\phi) \tag{55}$$

$$\rightarrow \frac{dQ}{dr} = B\rho r\Gamma(W\sin\phi + \epsilon W\cos\phi) = B\rho\Gamma(W_a + \epsilon W_t) \tag{56}$$

$$\rightarrow \eta = \frac{V}{\Omega r}\frac{(W_t - \epsilon W_a)}{(W_a + \epsilon W_t)} \tag{57}$$

The sectional propeller efficiency can with some additional work be subdivided into three efficiencies, an upstream efficiency η_{up}, and induced efficiency η_i, and a profile efficiency η_p:

$$\eta = \eta_{up}\eta_i\eta_p \tag{58}$$

$$\eta_{up} = \frac{1 - a'_\infty}{1 + a_\infty} \qquad \eta_i = \frac{1 - \frac{a'}{1 - a'_\infty}}{1 + \frac{a}{1 + a_\infty}} \qquad \eta_p = \frac{1 - \epsilon W_a/W_t}{1 + \epsilon W_t/W_a} \tag{59}$$

The upstream efficiency can go above 100%, if there is upstream swirl ($a'_\infty < 0$) or lower axial velocity. The induced efficiency goes towards 100% as the induction factors a and a' go towards zero. Profile efficiency is always below 100% except for the exceptional case where the airfoil procures no drag. For a minimum induced loss propeller that has a non-uniform inflow, the profile efficiency is ignored by setting $\epsilon = 0$ in equation (58):

$$\bar{\eta} = \eta_{up}\eta_i = \frac{VW_t}{\Omega r W_a} = \frac{VW\cos\phi}{\Omega r W\sin\phi} = \frac{V}{\Omega r\tan\phi} \tag{60}$$

$$\rightarrow r\tan\phi = \frac{V}{\Omega}\frac{1}{\bar{\eta}} = const. \tag{61}$$

In order for a propeller to be at the MIL condition it has to adhere to the Betz condition, which results in $\bar{\eta}$ (here called the induced efficiency from now on) being a constant, independent of radius.

3.3.10.2 Constraint equations and design algorithm

In order to reach an optimal design, the geometry needs to be changed until reaching a thrust target and maximizing efficiency. Two cases have been implemented, one for pre-specified chord and one for pre-specified c_l distribution. The set of constraint equations used are in the form of residual equations that are driven to zero with

different numerical schemes. There are two levels of residual equations, a global residual equation in order to reach desired thrust (or power), and local residual equations in order to reach desired chord or lift distributions.

Pre-specified chord	Pre-specified c_l
Global residual: $R_T = T(\bar{\eta}) - T_{spec} \to 0$ *or* $R_P = P(\bar{\eta}) - P_{spec} \to 0$ **Global variable:** $\bar{\eta}$ **Minimization routine:** Bisection method (interval halving)	**Global residual:** $R_T = T(\bar{\eta}) - T_{spec} \to 0$ *or* $R_P = P(\bar{\eta}) - P_{spec} \to 0$ **Global variable:** $\bar{\eta}$ **Minimization routine:** Bisection method (interval halving)
Residual for each radial position: $R_{\bar{\eta}} = \bar{\eta} - \frac{VW_t}{\Omega r W_a} \to 0$ **Local variable:** β **Minimization routine:** Newton-Raphson : $\delta\beta = -\frac{R_{\bar{\eta}}}{\partial R_{\bar{\eta}}/\partial\beta}$	**Residuals for each radial position:** $R_{\bar{\eta}} = \bar{\eta} - \frac{VW_t}{\Omega r W_a} \to 0$ $R_{c_l} = c_l - c_{l,spec} \to 0$ **Local variable:** c, β **Minimization routine:** Newton-Raphson: $\begin{bmatrix}\delta\beta\\ \delta c\end{bmatrix} = \begin{bmatrix}\frac{\partial R_{c_l}}{\partial\beta} & \frac{\partial R_{c_l}}{\partial c}\\ \frac{\partial R_{\bar{\eta}}}{\partial\beta} & \frac{\partial R_{\bar{\eta}}}{\partial c}\end{bmatrix}^{-1} \begin{bmatrix}R_{c_l}\\ R_{\bar{\eta}}\end{bmatrix}$

As an example, the pre-specified chord case is carried out as follows:

1. Set a starting value for $\bar{\eta}$ together with an initial geometry.
2. Calculate performance for the present geometry and the value of the residual $R_{\bar{\eta}}$, perturb β, calculate the derivative of $R_{\bar{\eta}}$, and calculate a new value for β. Iterate until it converges on a value for β and calculate the final thrust T.
3. Compare the obtained thrust with the target thrust, and increase $\bar{\eta}$ if the obtained thrust is too high, or decrease $\bar{\eta}$ if the obtained thrust is too low.
4. Go back to point 2 and iterate until $\bar{\eta}$ has converged too.

The case for pre-specified c_l is approached in a similar manner.

3.4 Methodology of Drela

Drela's methodology is based on having equal circulation Γ on the blade and in the wake, and therefore does not use any momentum equations.

3.4.1 Wake equations

The circulation bounded in a circle with radius r can be expressed with the average swirl in the wake $\bar{v}_t$, assuming that it behaves as a semi-infinite vortex sheet (explains the factor of 1/2):

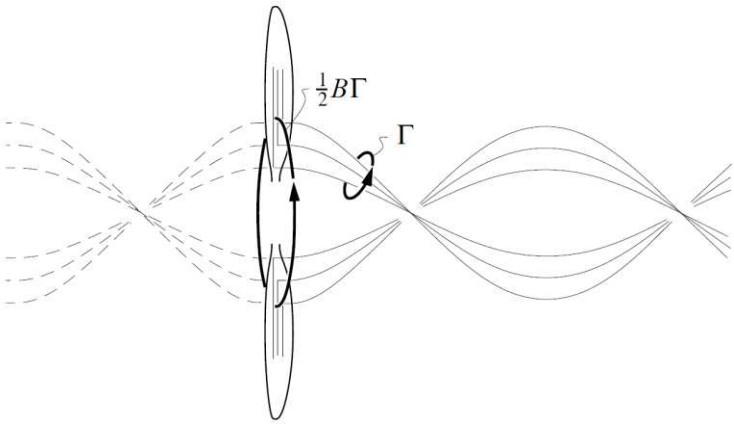

Figure 5 - The circuation present in a semi-infite vortex sheet. Source: Drela [7].

$$2\pi r\bar{v}_t = \frac{1}{2}B\Gamma \rightarrow \bar{v}_t = \frac{B\Gamma}{4\pi r} \tag{62}$$

Drela connects the average swirl at the wake $\bar{v}_t$ with the induced swirl on the blade v_t section with an **unreferenced** equation:

$$\bar{v}_t = v_t F\sqrt{1+\left(\frac{4\lambda_w}{\pi B\xi}\right)^2} \tag{63}$$

Drela also uses a different formulation for the Prandtl tip loss factor F:

$$F = \frac{2}{\pi}\text{acos}(e^{-f}) \qquad f = \frac{B}{2}(1-\xi)\frac{1}{\lambda_w} \qquad \lambda_w = \xi\tan\phi \tag{64}$$

Combining eq. (62) and (71), and solving for the induced swirl at the blade:

$$v_t = \frac{B\Gamma}{4\pi r}\frac{1}{F\sqrt{1+\left(\frac{4\lambda_w}{\pi B\xi}\right)^2}} \tag{65}$$

3.4.2 Blade section equations

Drela uses a clever parametrization of the velocities at the blade, illustrated in Figure 6. Drela's method takes into consideration the upstream induced velocities u_a and u_t to form intermediate velocities U_a and U_t:

$$U_a = V + u_a \quad \left(= V(1+a_\infty)\right) \tag{66}$$

$$U_t = \Omega r - u_t \quad \left(= \Omega r(1-a'_\infty)\right) \tag{67}$$

$$U = \sqrt{U_a^2 + U_t^2} \tag{68}$$

The velocities at the blade are written using the dummy variable ψ which varies with radius:

$$W_a = \frac{1}{2}U_a + \frac{1}{2}U\sin\psi \qquad W_t = \frac{1}{2}U_a + \frac{1}{2}U\cos\psi \qquad W = \sqrt{W_a^2 + W_t^2} \tag{69}$$

This allows the calculation of the circulation at the blade section with equation (43):

$$\Gamma = \frac{1}{2}Wcc_l \tag{70}$$

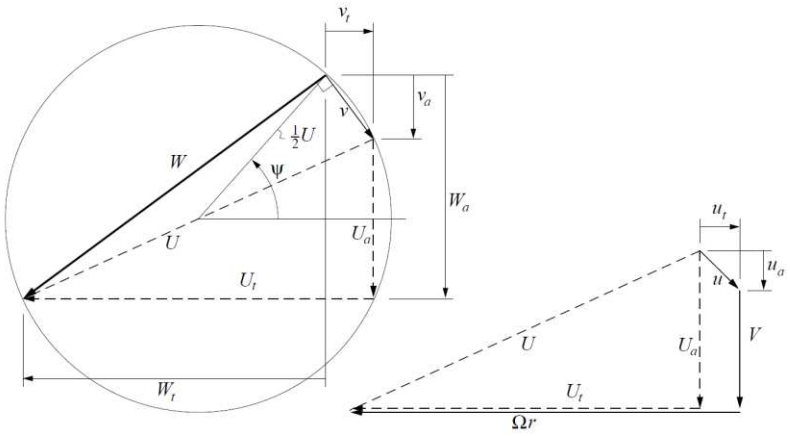

Figure 6 - Velocity parametrization used by Drela. Source: Drela (2006).

3.4.3 Drela analysis method

Drela's methodology is centered on analyzing an existing geometry, and the iterative algorithm is outlined below.

Drela design algorithm

1. Set an initial value for ψ.
2. Calculate the following expressions:

$$U_a = V + u_a \qquad U_t = \Omega r - u_t$$

$$U = \sqrt{U_a^2 + U_t^2}$$

$$W_a = \frac{1}{2}U_a + \frac{1}{2}U\sin\psi \qquad W_t = \frac{1}{2}U_a + \frac{1}{2}U\cos\psi$$

$$W = \sqrt{W_a^2 + W_t^2} \rightarrow Re, Ma$$

$$\phi = \operatorname{atan}\frac{W_a}{W_t} \rightarrow F$$

$$v_a = W_a - U_A$$

$$v_t = U_t - W_t$$

$$\alpha = \beta - \phi \rightarrow c_l, c_d, \epsilon$$

$$\rightarrow \Gamma = v_t \frac{4\pi r}{B} F \sqrt{1 + \left(\frac{4\lambda_w}{\pi B \xi}\right)^2}$$

$$R_\psi = \Gamma - \frac{1}{2}Wcc_l$$

3. The residual R_ψ is to be driven to zero for all radial positions by the means of a Newton-Raphson iteration. The derivative is calculated with finite differences after perturbing ψ and then updating R_ψ by going back to step 2.
4. After ψ has converged all relevant performance parameters such as dT/dr, T, η, etc. can be calculated.

3.4.4 Drelas design method

The design method for Drela follows exactly the same setup as the Capitao design method (Drela used this method first), and is explained in section 3.3.10.2. The only difference is that Drela's design method uses the Drela analysis method to evaluate designs.

3.5 SWIRL-CANCELLING RESIDUAL

In case the design target is to cancel out all possible swirl from an upstream device, then the performance (thrust, torque, efficiency, etc.) cannot be set as targets, but will instead be results from an iterative procedure similar to the two described in sections 3.3.10.2 and 3.4.4. The differences are:

- Removing the global residual on thrust/ power.
- Exchanging the residual $R_{\overline{\eta}}$ based on $\overline{\eta}$ to one based on the amount of induced swirl at the disk R_{swirl}. Note that a'_∞ is negative when coming from an upstream counter-rotating device.

Pre-specified chord	Pre-specified c_l
Residual for each radial position: $R_{swirl} = \frac{a'}{-a'_\infty} - 1 \to 0$ **Local variable:** β **Minimization routine:** Newton-Raphson : $\delta\beta = -\frac{R_{\overline{\eta}}}{\partial R_{\overline{\eta}}/\partial\beta}$	**Residuals for each radial position:** $R_{swirl} = \frac{a'}{-a'_\infty} - 1 \to 0$ $R_{c_l} = c_l - c_{l,spec} \to 0$ **Local variable:** c, β **Minimization routine:** Newton-Raphson: $\begin{bmatrix}\delta\beta \\ \delta c\end{bmatrix} = \begin{bmatrix}\frac{\partial R_{c_l}}{\partial\beta} & \frac{\partial R_{c_l}}{\partial c} \\ \frac{\partial R_{swirl}}{\partial\beta} & \frac{\partial R_{swirl}}{\partial c}\end{bmatrix}^{-1} \begin{bmatrix}R_{c_l} \\ R_{\overline{\eta}}\end{bmatrix}$

4 PROPELLER DESIGN CODE - OPTOPROP

4.1 OPTOPROP CODE STRUCTURE

The methods from section 3 have been implemented in the Matlab code OPTOPROP. The main structure of the code is displayed in Figure 7.

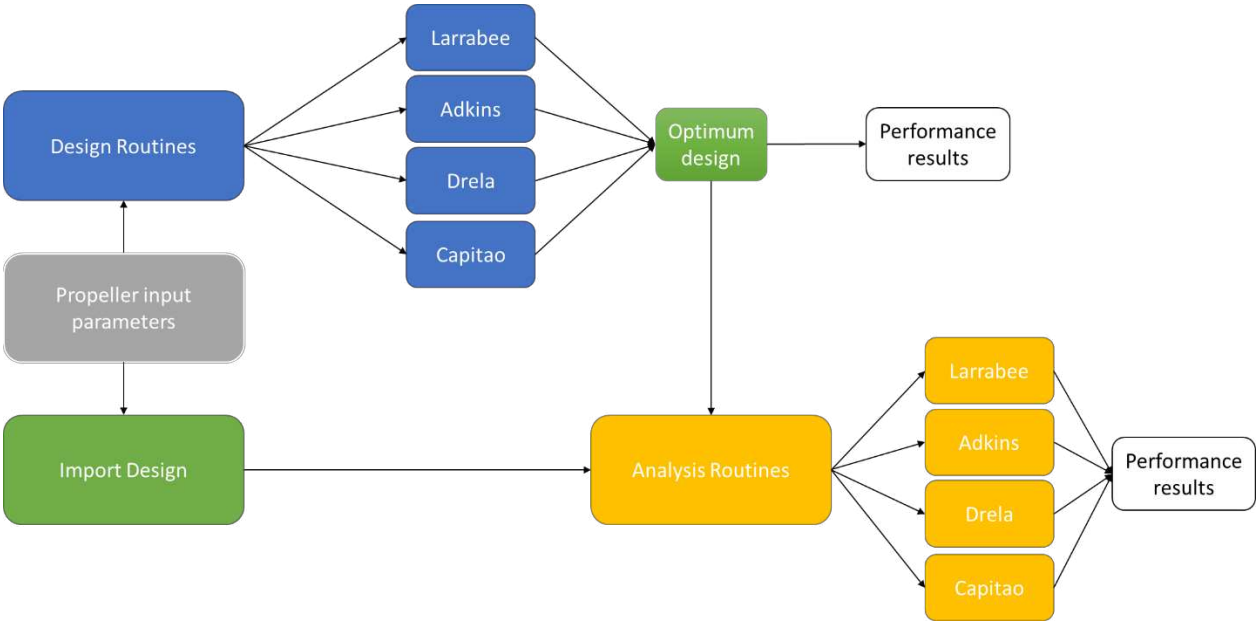

Figure 7 - OPTOPROP code structure.

The program can design propellers according to the minimum induced loss criterion or for swirl-cancellation. The obtained design can then be analyzed with any of the four analysis routines. The program can also analyze existing propeller blades by importing sectional properties such as chord, thickness, camber, blade angle, and airfoil sections.

For design and analysis the program needs the number of blades, diameter, hub-to-tip ratio (HTR), height above sea level, axial Mach number, rotational velocity, and upstream velocity profiles (for non-uniform inflow). For the design routines, there are power and thrust targets that need to be set.

For the cases of non-uniform inflow or swirl cancelling design condition only two design and analysis methods are applicable, namely the Drela and Capitao codes.

4.2 AIRFOIL TYPES

Three types of airfoil profiles have been implemented; an analytical Clark-Y profile, NACA-4415, and NACA-16 profiles. Post-stall models, Reynolds corrections, compressibility corrects have not been implemented.

4.2.1 Clark-Y

From reference [4] one can obtain a simple analytical expression for the sectional lift and drag coefficients for the CLARK-Y airfoil:

$$c_l = \kappa\alpha \qquad c_d = 0.006 + 0.010(c_l - 0.15)^2 \qquad \kappa = 6\ [c_l/rad] \tag{71}$$

4.2.2 NACA-4415

The paper by Adkins [6] includes a chart for the variation of c_l and c_d as function of angle-of-attack. Albeit of rough quality and without high accuracy, it has been digitized and is included in OPTOPROP.

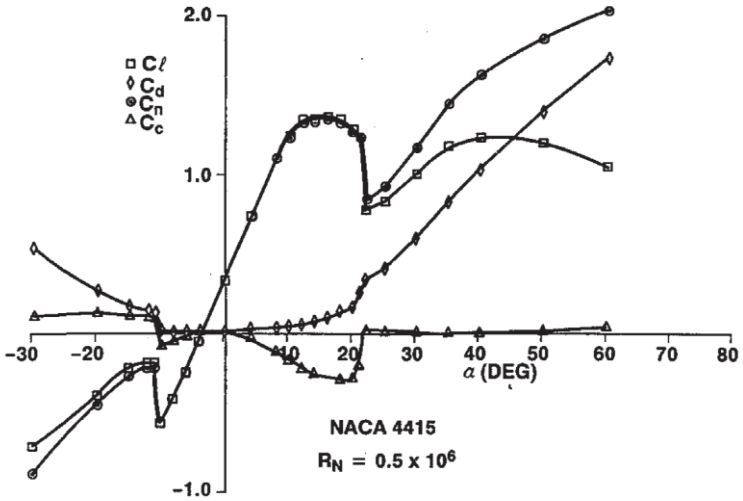

Figure 8 - NACA 4415 sectional properties.

4.2.3 NACA-16

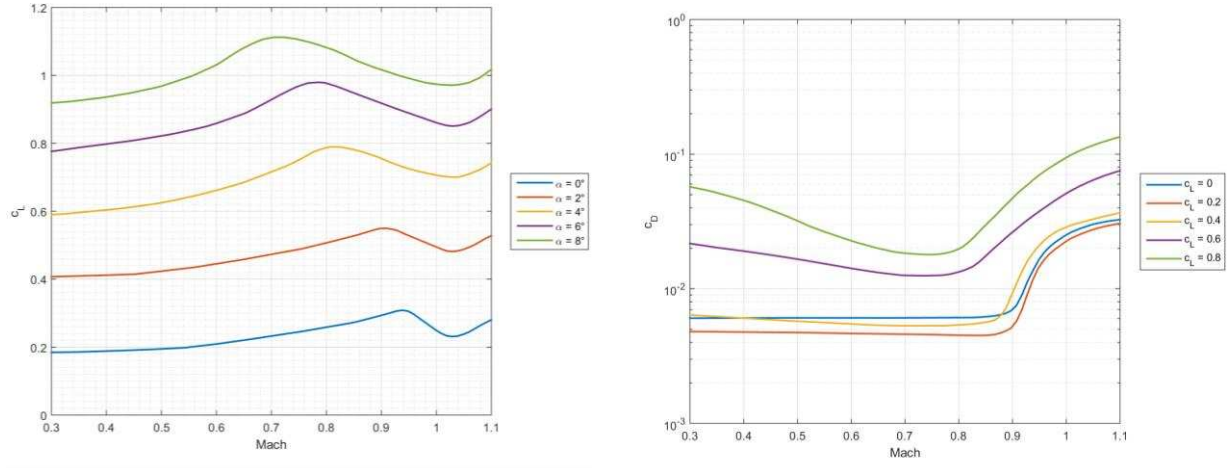

Figure 9 - NACA 16-204 sectional lift and drag coefficients as function Mach number and angle-of-attack.

The NACA-16 sectional properties have been included in an extensive report by Borst [12], and covers a large range of thicknesses, desing lift coefficients (camber), Mach numbers, and a limited amount of angle-of-attack values. For OPTOPROP, all sectional properties have been digitized for all thicknesses from 4% to 21%, design lift coefficients from 0 to 0.5, Mach numbers from 0.3 to 1.1, and angles-of-attack from 0 to 8 degrees. Unfortunately, this dataset is not complete, and therefore the following rules have been applied:

- If Mach number is below 0.3 or above 1.1, then the Mach number will be set to 0.3 and 1.1, respectively (nearest neighbor extrapolation). Any blade profiles operating outside the Mach number range will then get c_l and c_d values from the closest range limit.
- Coefficients of lift are extrapolated linearly outside the angle-of-attack range. This is not seen as a serious issue, since 8 degrees is a sufficient upper limit for most sections.
- Coefficients of drag are assumed to be symmetric with respect to angle-of-attack, and will therefore have the same drag coefficients for negative and positive angles-of-attack.

- Thicknesses above 0% and below 4% will be treated as 4% thick.
- Thicknesses above 21% are not allowed.

The program also warns if a propeller section is outside the ranges of the dataset.

5 RESULTS

5.1 MCCORMICK PROPELLER 5868-9

The propeller named 5858-9 is mentioned by McCormick [4] and the necessary information for its analysis can be found in a paper by Hartman [13] from 1938. This propeller was run in a NACA wind tunnel with constant rotational velocity, but varying axial velocity, in this way covering a range of advance ratios between 0 and 2.6. The whole blade pitch angle was also varied between 15 to 45 degrees. In this report, only the whole blade pitch angle of 45 degrees was used. More information on the propeller itself is presented below in Figure 10.

Number of blades:	*3*
Profile:	*CLARK-Y**
Diameter [m]:	*3.048*
Altitude [m]:	*0*
Rotational velocity [rpm]:	*1000*
Whole blade pitch angle [deg]:	*45*

**analytical expression*

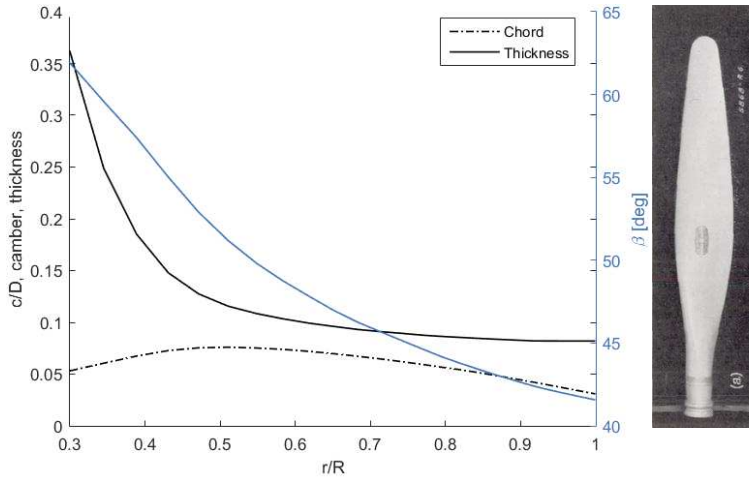

Figure 10 - Propeller sectional properties and planform (source: Hartman [13]).

The propeller design was analyzed with Larrabee's, Adkins', and Drela's methodologies and are presented in Figure 11 together with experimental data. All methods give decent results in the area of advance ratios between stall (low J) and below the area where the blade experiences negative angle of attack (high J).

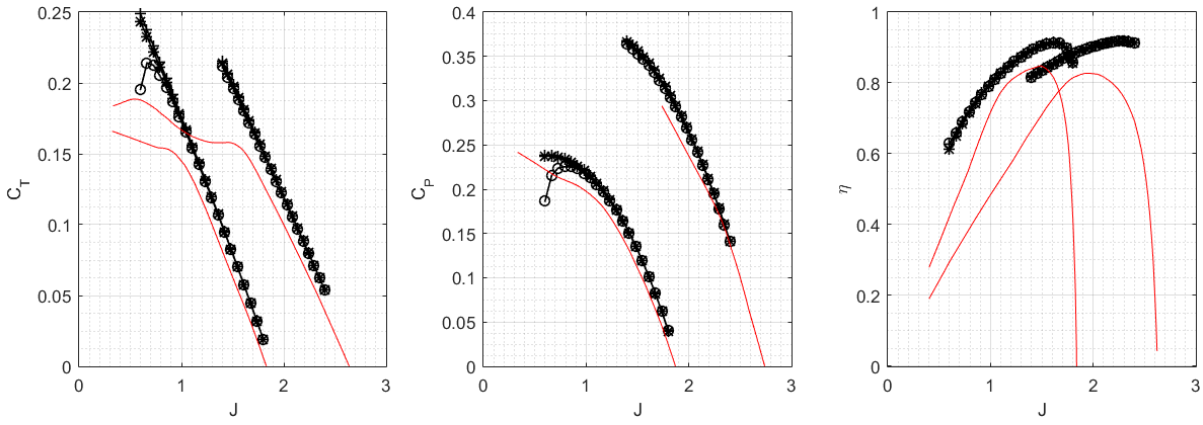

Figure 11 - Propeller performance for different advance ratios. The red lines represent experimental values, while the black lines represent analysis with different methods. The analysis methods return similar results.

5.2 LARRABEE PROPELLER

A propeller was designed with the same inputs as in the paper by Larrabee [5] in order to validate the Matlab implementation of the Larrabee design code in Matlab. The main design inputs are specified in Table 1.

Table 1 - Larrabee propeller design input

Diameter [m]:	1.829
Freestr. vel. [m/s]	53.64
Rot. vel. [rpm] :	2600
Design thrust [N] :	869.2
Drag-to-lift ratio:	0.025

Figure 12 – Obtained propeller planform

The obtained design was then analyzed with the Larrabee, Adkins and Drela analysis codes. The performance from the paper [5] is compared with other analysis methods in Table 2. The discrepancy between the Larrabee design and analysis routines is the fact that Larrabee uses small angle approximations in the design equations, leading to an inconsistency between design and analysis. As can be seen, the the Matlab implementation of the Larrabee code gives very similar results, except for a minor difference in efficiency.

Table 2 - Performance for design from the Larrabee paper [5] and the author's implementation of the Larrabee code. Results from the other implemented analysis routines are also included.

	Larrabee Paper	**Larrabee Design**	Larrabee Analysis	Adkins Analysis	Drela Analysis
$T[N]$	**869.2**	**869.2**	924.5	921.6	930.1
η [%]	**85.36**	**85.89**	85.74	85.68	85.79

5.3 ADKINS PROPELLER

The implementation of the Adkins methodology was also validated against the work of the original paper [6] in the same manner as the Larrabee propeller. The main design inputs are specified in Table 3, and for this case power is specified as design target rather than thrust.

Table 3 - Adkins propeller design input

Diameter [m]:	1.753
Freestr. vel. [m/s]	49.17
Rot. vel. [rpm] :	2400
Design power [kW] :	53.00
Profile:	$NACA$ 4415

Figure 13 - Obtained propeller planform

The performance from the paper [6] is compared with other analysis methods in Table 4. There is quite a large difference in efficiency relative to the paper, which is probably due to the bad quality of the image used to obtain the drag coefficient for the NACA 4415 profile. The drag coefficient is close to zero and very small compared to the lift coefficient (see Figure 8), which can lead to large errors in ϵ. In order to illustrate the sensitivity in the efficiency and thrust for varying c_d, a case has been run without any drag ($\epsilon = 0$) in Table 4. As can be seen in the table the results from the Adkins paper lies in the range between the Matlab implementation of Adkins' methodology with and without any drag. The similar results obtained with Larrabee's and Drela's methods support that the error might be in the airfoil sectional data. As promised by Adkins, the design and analysis methods give the same results.

Table 4 - Performance for design from the Adkins paper [6] and the author's implementation of the Adkins code. Results from the other implemented analysis routines are also included.

	Adkins Paper	**Adkins Design**	Larrabee Analysis	Adkins Analysis	Drela Analysis	**Adkins Design (no drag)**
$T[N]$	$\mathbf{923.5}$	$\mathbf{869.8}$	873.33	869.8	877.6	$\mathbf{960.2}$
η [%]	$\mathbf{86.996}$	$\mathbf{81.94}$	82.06	81.94	82.10	$\mathbf{90.46}$

5.4 REID PROPELLER

In the article by Adkins [6] there is a comparison between experiment and code for a propeller designed by NACA and published in an article by Reid [14]. The propeller is described in Figure 14.

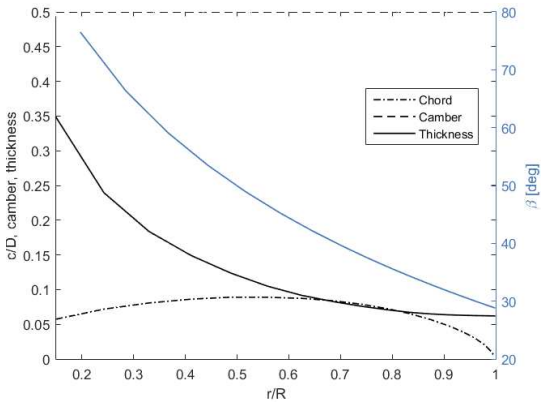

B	3
HTR	0.15
$D\ [m]$	0.8534
$Airfoil\ section$:	$NACA\ 16$

Figure 14 - NACA propeller model 5 properties.

This propeller geometry was analyzed in the Larrabee, Adkins, and Drela methods for three different blade angles $\beta_{0.75R}$, three rotational velocities, and advance ratios ranging from 0.2 to 1.8. The analyses are compared to experimental values in Figure 15. The analysis methods follows the trends relatively well, although the Adkins method collapses for lower advance ratios, where the blade stalls.

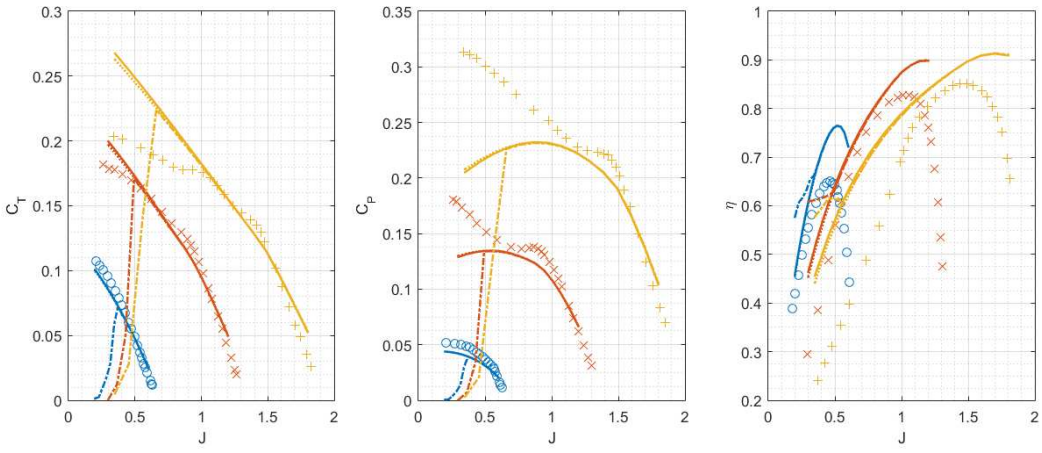

Figure 15 - Performance for the NACA Propeller Model 5. Continuous lines are values from the analysis methods, while points are experimental data. Blue represents $\beta_{0.75R} = 12°$, red represents $\beta_{0.75R} = 27°$, and yellow is $\beta_{0.75R} = 37°$.

5.5 GPS604 AND GPS609

Two existing, in-house propellers that have been simulated using CFD with free slip hubs were chosen to be analyzed with the different analysis methods. The operating conditions are described in Capitao Patrao [15]. Performance is compared for the two propellers in Table 5 and Table 6.

Table 5 - GPS604 performance comparison between CFD and different analysis methods.

GPS604	*CFD*	*Larrabe analysis*	*Adkins analysis*	*Drela analysis*
Thrust [N]	367.4	421.6	416.7	385.6
Efficiency [%]	76.34	76.28	76.16	75.12

Table 6 - GPS609 performance comparison between CFD and different analysis methods.

GPS609	*CFD*	*Larrabe analysis*	*Adkins analysis*	*Drela analysis*
Thrust [N]	387.4	394.5	390.3	361.5
Efficiency [%]	77.13	77.24	77.13	76.04

The CFD and analytical results compare rather well, especially for the GPS609 case. The sectional thrust profile for the two propellers is shown in Figure 16, where it can be seen that the propellers have different sectional thrust distributions relative to CFD, even if the global thrust is similar.

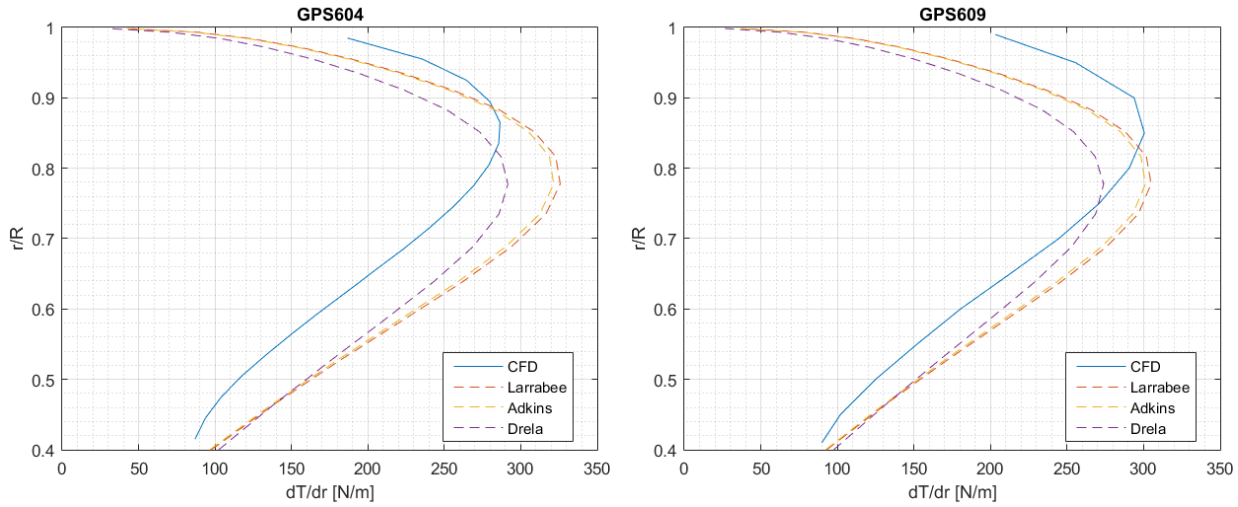

Figure 16 - Sectional thrust profiles for the GPS604 and GPS609 propeller blades for CFD and different analysis methods.

5.6 GPS621

The GPS621 propeller is a new 8-bladed propeller designed with OPTOPROP. Two variants were designed; one with Adkins' design methodology, and one with Drela's design methodology. The design parameters are specified in Table 7.

Table 7 – GPS621 design input parameters.

Diameter [m]:	0.75	*Chord dist:*	*SR7L*
Freestr. Mach nr.:	0.75	*Thickness dist:*	*SR7L*
Freestr. vel. [m/s]:	222.4	*Camber dist:*	*SR7L*
Rot. vel. [rpm] :	4997	*Airfoil profile:*	*NACA 16*
Design thrust [N] :	**333.2**		
Design C_T	**0.4**		

The design method also returns the performance of the design, which is tabulated together with the CFD values in Table 8. The sectional thrust is plotted in Figure 17. The designs did not reach the expected thrust levels, and some sort of calibration of the design methods might be needed.

Table 8 - GPS609 performance from the design methods and CFD simulations.

GPS609	*Adkins design perf.*	*Adkins design CFD perf.*	*Drela design. Perf.*	*Drela design CFD perf.*
T [N]:	333.2	268.8	333.1	299,9
P [kW]:	93.35	76.46	95.43	85,50
Efficiency [%]:	79.38	78.20	77.64	78,05

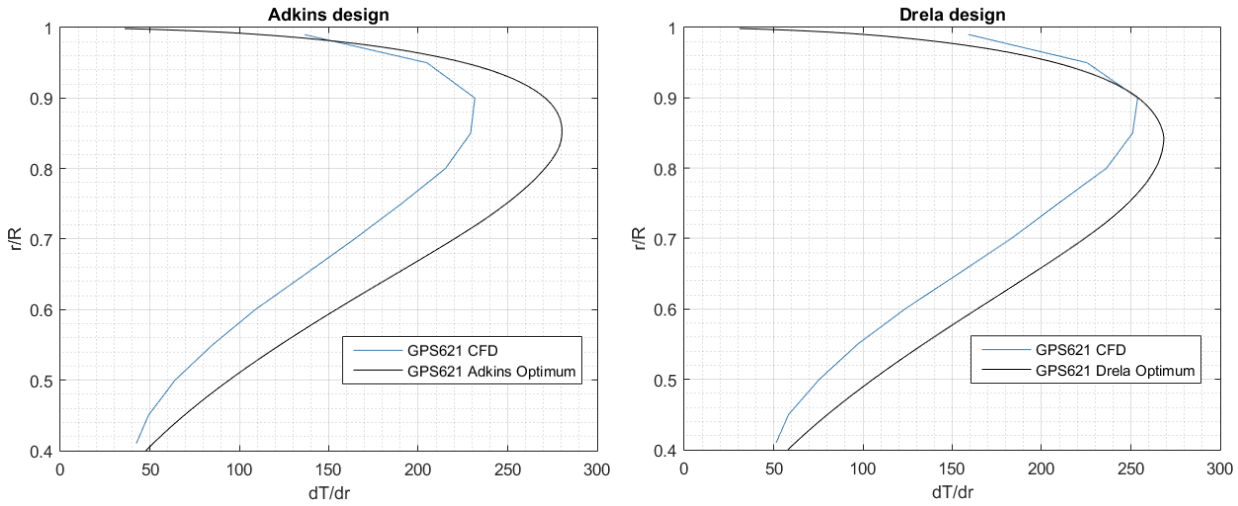

Figure 17 - Sectional thrust profiles for the GPS621 propeller blade designed with the Adkins and Drela methodologies. The thrust profiles are from the design process and from CFD simulations.

6 CONCLUSIONS

The aim of this work has been to review propeller design and analysis methodology, and to implement a propeller design code, OPTOPROP. This code can pave the way for future aero engine propeller research.

The developed propeller code has shown itself to be fast and quite capable of designing propeller and open rotor blades, but with slightly under-predicted thrust values. This can be overcome by re-designing the blades after analyzing the numerical results, specifically by adjusting the target thrust or power. Then the re-designed blades can be simulated numerically once again to check if the blades reaches target performance.

The capabilities of OPTOPROP will be used in the future for designing aero engine propellers, and its designs can potentially also be used to serve as baseline cases for more advanced optimization studies involving CFD.

7 REFERENCES

[1] Zondervan, G. J. D. "A review of propeller modelling techniques based on Euler methods." Series 01: Aerodynamics 05 (1998).

[2] Goldstein, Sydney. "On the vortex theory of screw propellers." Proceedings of the Royal Society of London. Series A, Containing Papers of a Mathematical and Physical Character 123, no. 792 (1929): 440-465.

[3]Theodorsen, Theodore. "The theory of propellers." (1948).

[4] Barnes, W., and W. McCormick. "Aerodynamics aeronautics and flight mechanics." (1995).

[5] Larrabee, E. Eugene. Practical design of minimum induced loss propellers. No. 790585. SAE Technical Paper, 1979.

[6] Adkins, Charles N., and Robert H. Liebeck. "Design of optimum propellers." Journal of Propulsion and Power 10, no. 5 (1994): 676-682.

[7] Drela, Mark. "QPROP formulation." Massachusetts Inst. of Technology Aeronautics and Astronautics, Cambridge, MA (2006).

[8] Béchet, Simon, Camil A. Negulescu, Vincent Chapin, and Frank Simon. "Integration of CFD tools in aerodynamic design of contra-rotating propellers blades." (2011).

[9] Negulescu, Camil A. "Airbus AI-PX7 CROR design features and aerodynamics." SAE International Journal of Aerospace 6, no. 2013-01-2245 (2013): 626-642.

[10] GONZALEZ-MARTINO, Ignacio, Benjamin FRANÇOIS, and Benoit RODRIGUEZ. "A physical insight into counter-rotating open rotor in-plane loads." 21ème Congrès Français de Mécanique, 26 au 30 août 2013, Bordeaux, France (FR) (2013).

[11] Kobayakawa, Makoto, and H. Onuma. "Propeller aerodynamic performance by vortex-lattice method." Journal of aircraft 22, no. 8 (1985): 649-654.

[12] Borst, Henry V. Summary of Propeller Design Procedures and Data. Volume 1. Aerodynamic Design and Installation. BORST (HENRY V) AND ASSOCIATES ROSEMONTPA, 1973.

[13] Hartman, Edwin P., and David Biermann. "The aerodynamic characteristics of full-scale propellers having 2, 3, and 4 blades of Clark y and RAF 6 airfoil sections." (1938).

[14] Reid, Elliot G. The influence of blade-width distribution on propeller characteristics. STANFORD UNIV CA, 1949.

[15] Patrao, Alexandre Capitao, Richard Avellán, Anders Lundbladh, and Tomas Grönstedt. "Wake and Loss Analysis for a Double Bladed Swept Propeller." In ASME Turbo Expo 2016: Turbomachinery Technical Conference and Exposition, pp. V001T01A013-V001T01A013. American Society of Mechanical Engineers, 2016.